1

Towards high performance anodes with fast charge/discharge rate for LIB based electrical vehicles

Hong Soo Choi and Chong Rae Park*
Carbon Nanomaterials Design Lab., Global Research Lab,
Research Institute of Advanced Materials,
Seoul National University (Department of Materials Science and Engineering)
Korea

1. Introduction

The increasing environmental problems nowadays, such as running out of fossil fuels, global warming, and pollution impact give a major impetus to the development of electrical vehicles (EVs) or hybrid electrical vehicles (HEVs) to substitute for the combustion engine-based vehicles. (Howell, 2008; Tarascon & Armand, 2001) However, full EVs that are run with electrical device only are not yet available due to the unsatisfied performance of battery. The automakers have thus focused on the development of HEVs, which are operated with dual energy sources, viz. the internal combustion heat of conventional fuels and electricity from electrical device without additional electrical charging process. As a transient type, the plug-in HEVs (PHEVs) are drawing much attention of the automakers since it is possible for the PHEVs to charge the battery in the non-use time. In addition, PHEVs have the higher fuel efficiency because the fuel can be the main energy source on the exhaustion of the battery.

Lithium ion batteries (LIBs) may be the one of the first consideration as an energy storage system for electrical vehicles because of higher energy density, power density, and cycle property than other comparable battery systems (Tarascon & Armand, 2001) (see Figure 1). However, in spite of these merits, the commercialized LIBs for HEVs should be much improved in both energy storage capacities such as energy density and power density, and cycle property including capacity retention and Coulombic efficiency in order to meet the requirements by U.S. department of energy (USDOE) (Howell, 2008) as listed in Table 1.

Figure 2 contrasts, on the basis of 40 miles driving range, the USDOE's performance requirements of the anode in LIBs for PHEVs with the performance of the currently commercialized LIBs (Arico et al., 2005). It is clearly seen that the power density of currently available anodes is far below the DOE's requirement although the energy density has already got over the requirement. Power density is the available power per unit time which is given by the following equation (1).

$$\text{Power density} = Q \times \Delta V \quad (1)$$

Here, Q is charge density (A/kg) which is directly related to the C/D rate, and ΔV is potential difference per unit time (V/s). This equation obviously shows that the higher power density can be achieved when the faster C/D rate is available. Therefore, the focus of the current researches for LIB anodes is on increasing the C/D rate and hence power density without aggravation of cycle property. Thus, we will limit the scope of this review to discussing the state of the art in the LIB anodes particularly for PHEVs.

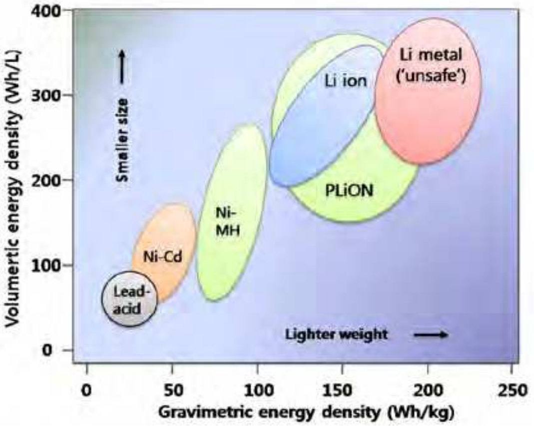

Fig. 1. Comparison of the different battery technologies in terms of volumetric and gravimetric energy density (Tarascon & Armand, 2001).

Characteristics at the End of Life		High Power /Energy Ratio Battery	High Energy /Power Ratio Battery
Reference Equivalent Electric Range	miles	**10**	**40**
Peak Pulse Discharge Power (2 sec/10 sec)	kW	**50/45**	**46/38**
Peak Region Pulse Power (10 sec)	kW	**30**	**25**
Available Energy for CD (Charge Depleting) Mode, 10 kW Rate	kWh	**3.4**	**11.6**
Available Energy in Charge Sustaining (CS) Mode	kWh	**0.5**	**0.3**
CD Life	Cycles	**5,000**	**5,000**
CS HEV Cycle Life, 50 Wh Profile	Cycles	**300,000**	**300,000**
Calendar Life, 35°C	year	**15**	**15**
Maximum System Weight	kg	**60**	**120**
Maximum System Volume	Liter	**40**	**80**
System Recharge Rate at 30°C	kW	**1.4 (120V/15A)**	**1.4 (120V/15A)**
Unassisted Operating & Charging Temperature	°C	**-30 to +52**	**-30 to +52**
Maximum System Price @ 100k units/yr	$	**$1,700**	**$3,400**

Table 1. USDOE's battery performance requirements for PHEVs (Howell, **2008**)

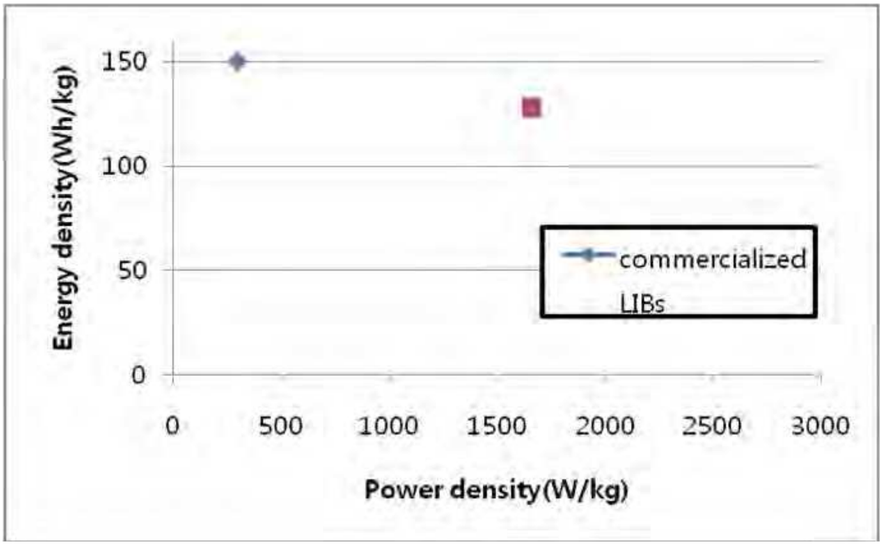

Fig. 2. Energy storage performance of the commercialized LIBs and the USDOE's goal.
*Each energy density and power density of the goal from DOE is calculated on the basis of 40 mile run of PHEVs. The mass of anode is assumed to be 25 % of whole battery mass, and ratio of active material in the anode is assumed to be 80% of anode mass. Working voltage of the batteries is assumed to be 3V.

2. Performance deterioration of the carbon anodes with fast C/D rate

2.1 Performance limitation of carbon anodes for electrical vehicles

The commercial anode material of LIBs is carbon materials, which have replaced the earlier lithium metal and lithium-metal composites, and categorized into graphite, hard carbon and soft carbon with a crystalline state. (Julien & Stoynov, 1999; Wakihara, 2001) Most widely used carbon-based material is graphite that is cheap, and has high Coulombic efficiency and 372 mAh/g of theoretical specific capacity (Arico et al., 2005). The C/D process of the graphite anode is based on the intercalation and deintercalation of Li ions with 0.1~0.2 V of redox potential (Wakihara, 2001). This C/D mechanism can be a basis of the cell safety, because the intercalated Li ions are not deposited on the surface of the graphite anode preventing dendrite formation during charging process. The intercalation of Li ions between graphene galleries provides a good basis for excellent cycle performance due to a small volume change. Also, 0.1~0.2 V of Li^+ redox potential, close to potential of Li metal, contributes to sufficiently high power density for electrical vehicles.

However, as can be seen in Figure 3, untreated natural graphite shows capacity deterioration with increasing cycle numbers, particularly as the charging rate increases. On the application of LIBs to PHEVs, this capacity deterioration with fast C/D rate can be detrimental because the battery should survive fast C/D cycles depending on the duty cyles such as uphill climbing and acceleration of the vehicle.

There have naturally been a variety of researches to overcome the weakness of graphite anode or to find substitute materials for graphites. Before introducing such research activities, below are briefly reviewed the origins of capacity deterioration with fast C/D rate of graphites and/or graphite based composite anodes.

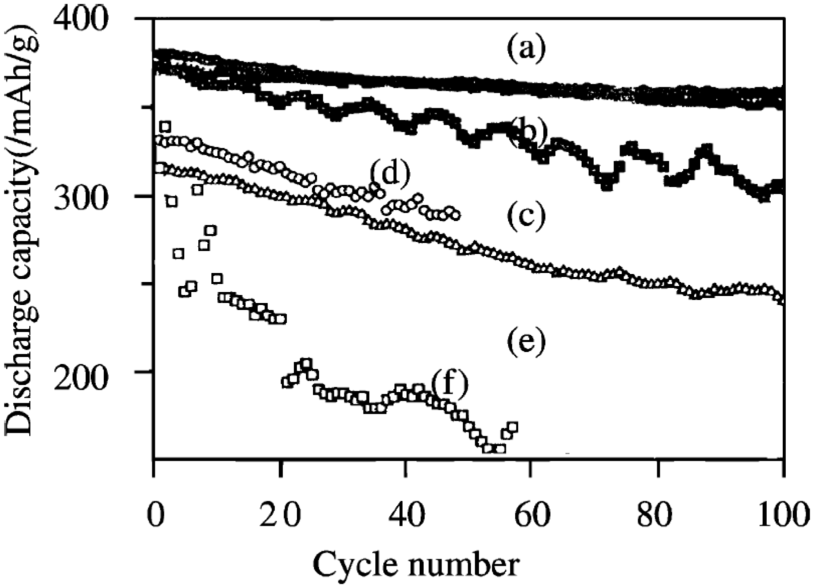

Fig. 3. Cycling performance of natural graphite (curves d, e and f) and Al-treated sample (curves a, b and c): circles, triangles and rectangles represent 0.2 C, 0.5 C and 1 C rate, respectively. (Kim et al., 2001)

3. Origins of performance deterioration of the graphite anode with fast C/D rate

The electrochemical performance of the anode material of LIBs is best described by Nernst equation of half-cell reaction as shown by equation (2). (Bard & Faulkner, 2001) A general half-cell reaction on the surface of the active material of the anode is

$$v_O O + ne \rightleftharpoons v_R R \tag{2}$$

where v_O and v_R are stoichiometric coefficients for oxidant and reductant, respectively, in this reaction. At equilibrium, the energy obtainable from equation (2) is given by the passed charge times the reversible potential difference. Therefore, the reaction on the surface of the active material in the anode is described by equation (3)

$$\Delta G = -nFE \tag{3}$$

where ΔG is Gibbs free energy of the reaction, n is the number of the passed electrons per reacted Li atom, F is the charge of a mole of electron (about 96500 C), and E is electromotive force (emf) of the cell reaction. This equation highlights the kinetic nature of electron transportation, being expressed by E of the electrostatic quantity, and the thermodynamics nature of redox reaction of Li ions, ΔG.

Based on equation (2), the following equation (4) can be developed.

$$E_{anode} = E_{anode}{}^{0} - \left(\frac{RT}{nF}\right) \ln \frac{A_{anodic}}{A_{cathodic}} \tag{4}$$

Here, E_{anode} and $E_{anode}{}^{0}$ are the anode half-cell potential and standard half-cell potential, respectively, R is the ideal gas constant (8.314 $J/molK^{-1}$), and A_{anodic} and $A_{cathodic}$ are the chemical activities of anodic and cathodic reactions, respectively.

The C/D process of LIBs, as shown in Figure 4, includes (1) the redox reactions on the surface of the electrodes and (2) charge (including both ions and electrons) transfer process.

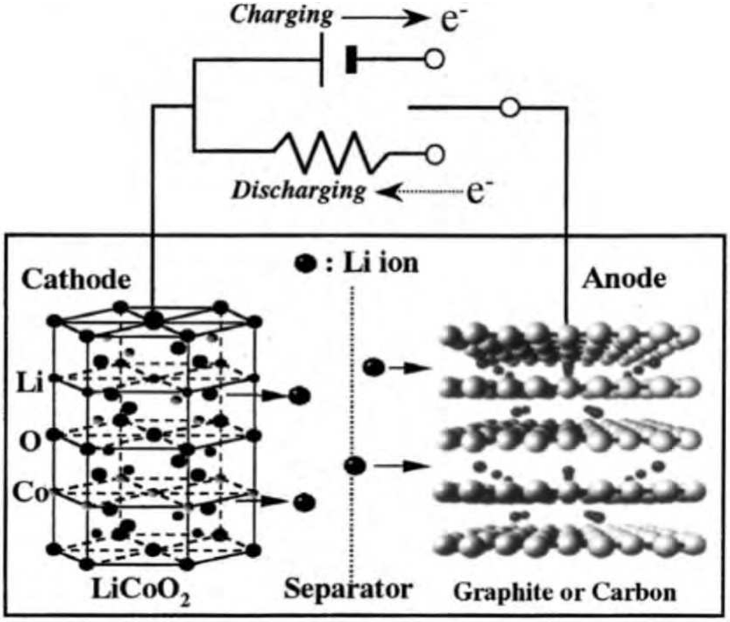

Fig. 4. Charging-discharging mechanism of Li ion secondary battery (Endo et al., 2000).

Basically, based on generally accepted assumption of negligible mass transfer in the electrolyte due to the presence of excess supporting electrolytes in the LIBs, the rate of charge transfer on the surface of the electrode can be generally described with the Butler-Volmer equation (Bard & Faulkner, 2001; Julien & Stoynov, 1999) (equation 5) that contains the natures of both electrons and ions although the detail mechanism is slightly different with kinds of active materials: for example, diffusion and intercalation of Li ions for graphite (Endo et al., 2000) whereas diffusion and alloying for elemental metals (Tarascon & Armand, 2001).

$$i = i_0 \left[e^{\alpha_O f \eta} - e^{-\alpha_R f \eta} \right] \tag{5}$$

where i_0 is exchange current, which indicates the zero net current at equilibrium with Faradaic activity, α_O and α_R are transfer coefficient of oxidation and reduction reactions, respectively, indicating the symmetry of the energy barrier, f=F/RT (F : Faraday constant), and η (=E-E_{eq}) is overpotential, being the measure of the potential difference between thermodynamically determined potential at equilibrium (E_{eq}) and experimentally measured redox potential (E) due to electrochemical reaction with electrons and ions.

The equation itself shows clearly that to enhance C/D performance of LIB anodes the kinetics of electron and ion transportation on and/or in the anode material should be improved.

3.1 Important factors influencing the C/D performance of LIB carbon anodes

The practical LIB system consists of active materials, e.g. graphites, conducting materials, e.g. carbon black, and binder materials, e.g. polyvinylidenefluoride (PVDFs). In this kind of structure the kinetics of electron and ion transportations is influenced by many different factors. From a viewpoint of electron transportation, the movements of electrons from current collector to active materials and from the surface to the inside the active materials are crucial. In this sense, the electron conductivities of the conductive materials including carbon blacks and active materials connected by the binder including PVDFs become very important factors determining the C/D performance of LIB anodes.

On the other hand, Li ions move from the cathode through electrolytes to the surface and then diffuse into the graphites. It is therefore very important that the electrolytes and the active materials should have excellent ion conductivity to minimize the internal resistance of the cell. However, the ionic conductivity of the electrolyte used in practical LIBs is about 10^{-2} S/cm, which is quite lower value than that of aqueous electrolytes. (Wakihara, 2001) Moreover, as the reduction reaction of Li ions occurs on the surface of the active materials the physico-chemical nature of the active materials is another important influencing parameter on the C/D performance of the LIB anodes.

The fabrication factors of the anode, for example, mixing ratio, thickness of electrode, and etc., can also influence the kinetics of electron and ion transportation because these variables affect the formation of percolation pathway of electrons and/or ions. Indeed, Dominko et al. (2001) showed that good contact between each component materials of the electrode, which was achieved by homogeneous distribution of carbon blacks, is an important factor for the performance of LIBs as shown in Figure 5.

In the case of fast C/D rate circumstance as in electrical vehicles whereby rapid charge transfer occurs, the above-mentioned fabrication variables may become important factors, although those are negligibly small in slow rate C/D process. However, to avoid the diversion of the present review, we will limit our discussion on the influential factors directly related to the active materials themselves.

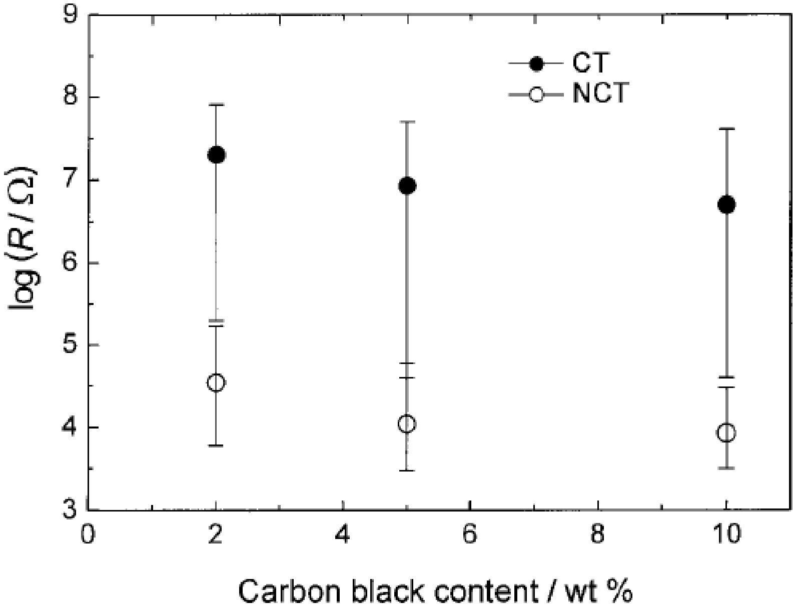

Fig. 5. Dependence of microcontact resistances (R) around active particles on carbon black content. Each bar represents the span of many (10~20) resistance measurements on various particles on the surface of the same pellet. Circles represent average values of the given series. (Dominko et al., 2001)

3.2 Origin of performance deterioration of carbon anodes with fast C/D rates

Despite that a fast rechargeable performance is one of the most important properties required for electrical vehicles the presently available commercialized LIBs show a poor performance in the fast charge/discharge circumstances. For example, the graphite anode shows decay in the specific capacity to ~350 mA/g at over 1C C/D rate (see Figure 3). We will briefly deliberate on the possible origins of this performance deterioration of carbon anodes with fast C/D rates.

3.2.1 Poor electron transportation with fast C/D rates

In the case of fast C/D process, the electron transportation can be influenced by different factors from those for normal or slow C/D rates. For example, poor electron transportation in the anode may arise from three different origins, viz. (1) contact problem between the current collect and the electrode component, (2) low electronic conductivity of the electrode components, and (3) low electronic conductivity of active material.

(1) Poor contact at the interface of the electrode

There are two kinds of the concerned interfaces in the LIB electrodes, viz. the interfaces between the current collect and the electrode components and between the components of the electrode. Since these interfaces play a role of electron transportation pathway, good contact at the interfaces can lead to excellent cell performance. In particular, under a fast C/D process, there can be a large volume deformation of the active materials, which originates from lithiation and delithiation. If there exists a hysteresis in the volume deformation, then the interfacial contact cannot be ensured, which directly leads to deterioration of the electrode performance. Indeed, as can be seen in Figure 6, this phenomenon is common to the case of elemental metal electrodes, such as Si, Sn, and Sb, even under slow C/D rate circumstances. (Julien & Stoynov, 1999)

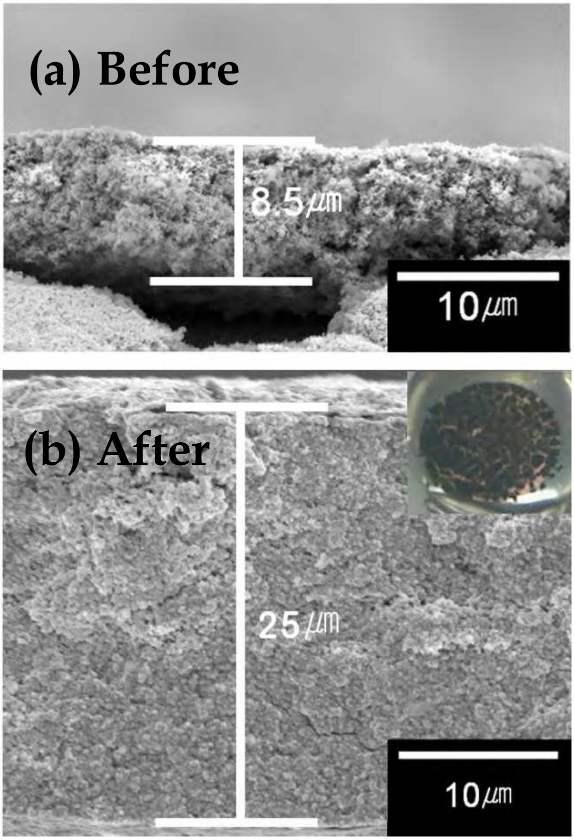

Fig. 6. The volume deformation before (a) and after (b) 1 cycle of C/D process with 50 mA/g charging rate and the resultant cracks (inset of (b)) of the Si-nanoparticle based anode.

In the case of carbon anodes, the volume deformation is not so big as that of metallic anode but still an influential factor of the fast C/D performance. (Yazami, 1999)(also see Figure 3.) Figure 7 illustrates the expansion of the space between graphene sheets during C/D process and the formation of thin film on the surface of graphites due to the deposition of electrolyte decomposition products (Figure 7(b), and the resultant performance deterioration (Figure 7(a)). (Besenhard et al., 1995)

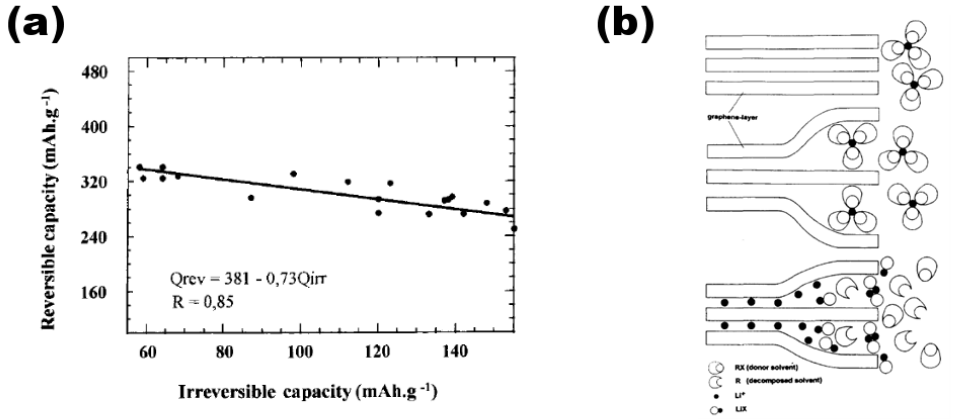

Fig. 7. (a) Q_{rev} vs. Q_{irr} linear dependence for Li/1 M $LiPF_6$; EC(1):DMC(1):DME(2) /Graphite cells under cycle rate of 0.2C at the ambient temperature. (Yazami, 1999) (b) Schematic illustration of the film forming mechanism via decomposition of $Li(solv)_yC_n$. (Besenhard et al., 1995)

(2) Low electronic conductivity of the component materials of carbon anode

The electronic conductivity (κ) of the graphite anode system can be generally described by the following equation (Bard & Faulkner, 2001)

$$\kappa = F\sum |z_e| u_e C_e \qquad (6)$$

where z_e is the charge of electron, u_e is the mobility of electron, and C_e is the concentration of electron. As predicted by equation (6), the electronic conductivity is directly related to the electron mobility in the system, which varies with many factors such as morphology and surface nature of the active material. In most of commercial carbon anode systems, granular graphites of which electronic conductivity is about 10^{-1}~10^{-4} S/cm are intermixed with conducting carbon blacks of the conductivity of about 10^{-2} S/cm (Brett & Brett, 1993) and polyvyniliden fluorides (PVDFs) that have the conductivity of about 10^{-13} S/cm (Ji & Jiang, 2006). It is therefore necessary to considerably improve the electronic conductivity of the component materials of carbon anodes. Table 2 shows the electronic conductivity of various carbon materials used in the commercialized LIBs.

3.2.2 Poor ionic transportation in the carbon anode with fast C/D rate

As with the issue of electron transportation, the ionic conductivity is a counter factor governing the performance deterioration with fast C/D rate. During C/D process of LIBs, Li ions travel from the cathode via electrolytes to the surface of the anode. The efficiency of the electrode performance is therefore strongly influenced by the efficiency of the charge transfer from one to another component material of the electrode as described by Butler-Volmer equation. Especially, under fast C/D rate conditions, the ions have to transfer fast enough to maximize its partition to the redox reactions on the anode surface. In this sense, the electrolytes should have excellent charge transfer efficiency. Also, after reaching of the ions to the anode surface, the effective participation of the ions to the redox reaction is governed by the physico-chemical surface nature of the carbon active material.

	Resistivity (Ω.cm)
HOPG (highly ordered pyrrolytic graphite), a-axis	4 X 10^{-4}
HOPG (highly ordered pyrrolytic graphite), c-axis	0.17
Randomly oriented graphite (Ultracarbon UF-4s grade)	1 X 10^{-3}
Carbon black (Spheron-6)	0.05

Table 2. Electronic conductivity of various carbon materials (Brett & Brett, 1993)

Basically, the ionic charge flux in an electrolyte can be described by equation (7) because Li ions far away from the electrode migrate by mass transfer mechanism due to almost zero concentration gradient in bulk solution.

$$J_{Li^+} = |z_i| F u_i C_i \frac{d\Phi}{dx} \tag{7}$$

where z_i is the charge of Li ion, F is Faraday constant, u_i is the mobility of Li ion, th term of $F \times u_i = \kappa$ is the ionic conductivity in the electrolyte, C_i is the concentration of Li ions, and $d\Phi/dx$ is the potential difference between the electrodes. That is, in a given LIB system, the Li ion flux depends on the Li ion concentration and the ionic conductivity in the electrolytes. In actual uses of LIBs, excess amount of nonelectroactive supporting electrolyte, for example $LiBF_6$, is being used in order to minimize ionic mass transfer by migration and concurrently to maximize the charge transfer by diffusion. This excess supporting electrolyte helps to decrease the solution resistance and improve the accuracy of working electrode potential, and consequently guarantees an uniform ionic strength irrespective of some fluctuation in the amount of ions. (Bard & Faulkner, 2001) To achieve fast ionic transfer in the electrolyte, it is therefore important to secure a continuous ionic pathway to the surface of active materials in the anode system.

On the surface of the active material, graphite, the kinetics of surface positive charge transfer follows Butler-Volmer equation. This kinetics also follows diffusion migration theory due to the uses of supporting electrolyte and ultramicroelectrode (UME) of small-sized active materials. At a steady state or a quasi-steady state of UMEs, the surface current of UMEs can be described by equation (8). (Bard & Faulkner, 2001)

$$i = nFAm_iC_i \tag{8}$$

Here, A is the surface area of the UME, m_i is the mass transfer coefficient, and C_i is the ionic concentration on the surface of the UME. As the surface area, A, and the mass transfer coefficient, m_i, vary with morphology of UMEs, it is important to control shape and size of the active materials so that the shortest charge diffusion path can be ensured. Indeed, the charge transfer time per each Li ion in the electrode, T, is directly related to the diffusion path (d_i) as shown in equation (9), being based on the interstitial diffusion. (Bard & Faulkner, 2001; Porter & Easterling, 1991)

$$T=\frac{d_i^2}{\alpha^2 D_i} \tag{9}$$

Here, D_i is the diffusion coefficient of Li ion and α is the number of available vacant interstitial sites in the active material lattice, of which number varies with the micro-structure of the active material.

From the above-mentioned theoretical consideration, we can conjecture two approaches to maximizing ion transportations: one is to ensure effective ionic pathways to the active materials in the anode and the other is to increase the ionic transfer rate on and in the active materials. These two goals can be achieved by (1) morphology control and (2) surface modification of the active materials, and (3) appropriate fabrication to ensure homogeneous distribution and good interfacial contact of conducting materials and the active materials in the anode system. The recently developed nanostructured active materials are expected to be effective for high rate of ionic transfer due to huge 'surface area/volume' ratio and short ionic diffusion path. However, many researches using nanoparticles, for example Si nanoparticles (Wang et al., 2004), proved that this approach is not always working because the nanostructured materials tend to aggregate each other, leading to decreasing of accessible surface areas to electrolytes.

4. Strategies for the material-design of high performance anode with fast C/D rate

In order to achieve good anode performance with fast C/D rate of LIBs for PHEVs, a variety of approaches have been proposed. Below are described the strategies of those researches, most of which are concerned with the aforementioned fundamental issues, viz. the enhancement of electron transportation kinetics and the achievement of high ionic conductivity in the electrode system.

4.1 To enhance the kinetics of electron transportation

The works on the enhancement of electron transportation kinetics can be categorized into three groups: one group is on the morphology control of active materials, another on the surface modification of active materials, and the other on the synthesis of hybrid and/or composite anode materials.

4.1.1 Morphology control of the active materials

To have short diffusion path and high transportation rate of electrons without substitution or additional treatment of the active material, morphology control techniques have been adopted (Chan et al., 2008; Cho et al., 2007; Fang et al., 2009; Hu et al., 2007; Kim et al., 2006; Lampe-Onnerud et al., 2001; Park et al., 2007; Subramanian et al., 2006; Takamura et al., 1999; Tao et al., 2007; Wang et al., 2009; Wang et al., 2008; Zaghib et al., 2003) to fabricate 1D fibrous structures, 2D sheets or films, and 3D porous or specified structures of the active material (Tao et al., 2007). The commercialized graphites are of spherical shape whereby 2D-

laminate structure works for intercalation of Li ions in C/D process. (Endo et al., 2000; Tarascon & Armand, 2001; Wakihara, 2001; Wu et al., 2003) In recent, extensive researches have been expended to finding possible ways of utilizing graphenes as a new class of 2D structure anode material due to its impressive electrical properties. (Makovicka et al., 2009; Nuli et al., 2009; Wang et al., 2009; Yoo et al., 2008)
Generally, 1D fibrous structure is considered an effective system which strengthens the interfacial contacts in the anode system. (Cho et al., 2007; Kim et al., 2006; Xia et al., 2003) For instance, silicon nanowires directly grown on the current collector can enhance the LIBs anode performance under high C/D rates. Figure 8 illustrates that the 1D Si nanowires have the capacity of about 2000 mAh/g even at 1C rate (about 4200 mA/g of C/D rate), arising from the efficient electron pathway secured from good interfacial contact between 1D Si nanowires and the current collector. (Chan et al., 2008) The carbon nanofiber network was also found to exhibit good anodic performance at high C/D rates, (Kim et al., 2006) which originates from good interfacial contacts between the component materials of the anode system and also between the active materials ensuring effective electronic conductivity.

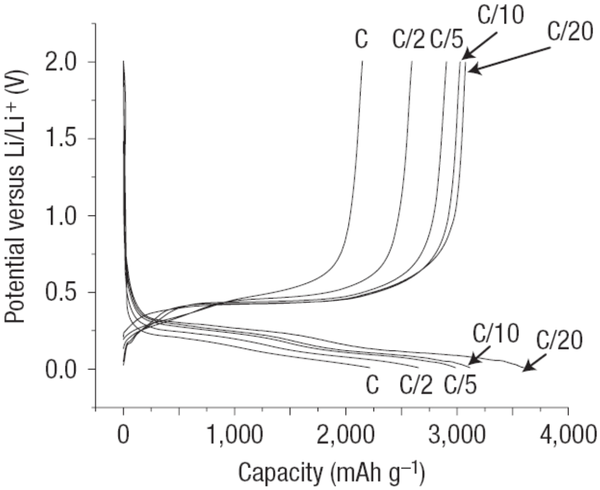

Fig. 8. The voltage profiles of Si nanowires at various C/D rates. (Chan et al., 2008)

In recent, representative 2D carbon structure, graphenes are receiving spot lights due to a large surface to volume ratio and high conductivity. Wang et al. (2009) synthesized graphene nanosheets by reducing graphite oxide and tested anodic performance under 1C C/D rate (about 700 mA/g). The graphene anode indeed exhibited excellent anodic performance at high C/D rate, viz. about 460 mAh/g of reversible specific capacity until 100th cycle as shown in Figure 9.

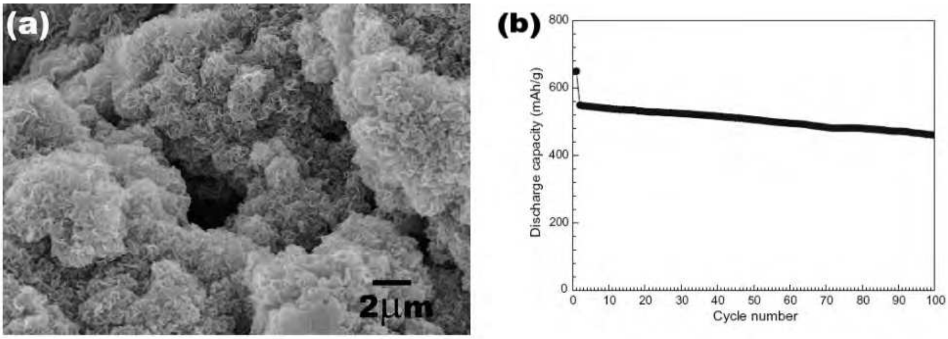

Fig. 9. FE-SEM image of loose graphene nanosheets (a) and discharge capacity (lithium storage) of graphene nanosheet electrode as a function of cycle number at 1C (about 700 mA/g). (Wang et al., 2009)

As for 3D structured anode materials (Tao et al., 2007), porous 3D structure was reported to be helpful to connect the electron pathway effectively. (Long et al., 2004) For example, hierarchical porous carbon structure showed very impressive anodic performance at high C/D rate (Hu et al., 2007) (see Figure 10). This level of anodic performance at high C/D rate is thought to be possible due to good electron pathway and effective Li ions transport via channel-like pores.

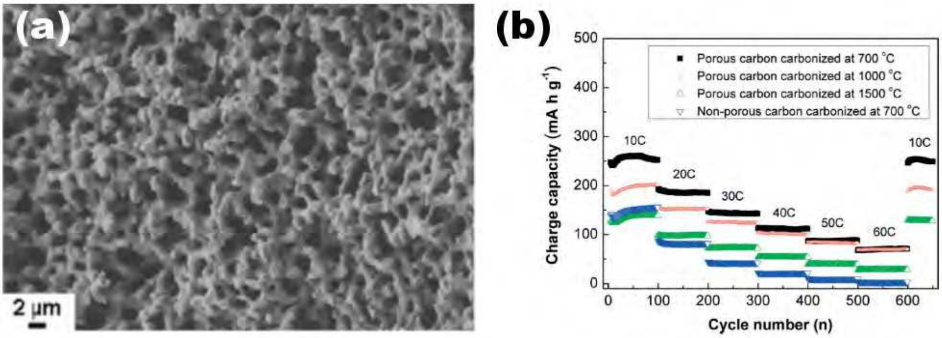

Fig. 10. SEM image of nanocast carbon (carbonized at 700 °C) replica (a) and rate performance of the porous carbon samples carbonized at different temperatures and non-porous carbon from mesophase pitch (carbonized at 700 °C). (Hu et al., 2007)

4.1.2 Surface modifications of active materials

Another way of enhancing electron transportation in the anode system is through surface modifications which are categorized into two groups: one is to coat conducting material on to the surface of the active materials and the other is to dope heteroatoms into metallic oxide anodes to increase electronic conductivity.

(1) Coating of conducting material

To coat conducting material is one of the most widely used surface modifications to enhance the high rate capability of the LIBs anode materials. There are two kinds of mainly adopted conducting materials, viz. carbon materials (Dominko et al., 2007; Kim et al., 2009; Kim et al., 2009; Lou et al., 2009; Sharma et al., 2003; Wang et al., 2007; Zhang et al., 2008) and various metals and their oxides (Choi et al., 2004; Fu et al., 2006; Guo et al., 2002; Kottegoda et al., 2002; Nobili et al., 2008; Takamura et al., 1999; Veeraraghavan et al., 2002; Wang et al., 2003; Zhang et al., 2007), such as Al, Au, Ag, Co and Cu. In the case of carbon materials, hydrothermal reaction and gas phase reaction of various organic carbon precursors, for instance, citrate (Dominko et al., 2007), sugar (Wang et al., 2007), glucose (Zhang et al., 2008), ethylene glycol (Kim et al., 2009), Super P MMM carbon (Sharma et al., 2003), and propylene(Kim et al., 2009), have been used to introduce the carbon coating on the surface of the active materials. In the case of metal coating, CVD method and evaporation method have been mainly used due to easy controllability of the properties of the coated metals.

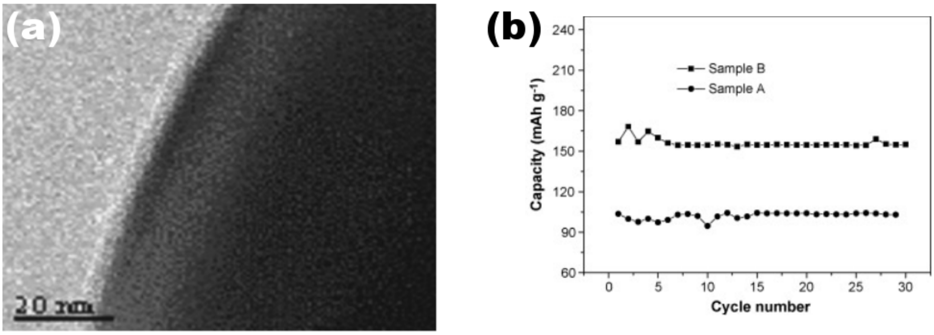

Fig. 11. TEM image of carbon-coated (a) and the relationship of the reversible capacity of the virgin (sample A) and carbon-coated $Li_4Ti_5O_{12}$ (sample B) at 0.1 C with cycle number (b). (Wang et al., 2007)

Carbon coating has been usually applied to metal or metal oxide anodes to give good electronic conductivity and stability as well as barrier property to the formation of SEI layer (Cui et al., 2007; Derrien et al., 2007; Zhang et al., 2008). For example, $Li_4Ti_5O_{12}$ has been considered as an attractive anode candidate for HEVs or EVs because of stable theoretical specific capacity of approximately 170 mAh/g and zero strain and negligible volume deformation during C/D process. This material exhibits however poor C/D performance at high rates due to very low electronic conductivity of about 10^{-13} S/cm (Dominko et al., 2007). The carbon coating on this $Li_4Ti_5O_{12}$ increased twice as high as the specific capacity at 0.1C C/D rate than uncoated one (see Figure 11). The carbon-coated SnO_2 nanospheres also showed much enhanced specific capability of 200 mAh/g at 3000 mA/g C/D rate. (Lou et al., 2009) In this case, carbon layer additionally prevented volume expansion of SnO_2 by over 250 %.

Metal coating guarantees the faster charge transfer on the surface of the active materials due to high electronic conductivity of metals. In addition, SEI layers on the coated metals, especially, Cu and Sn, have lower resistivity and higher Li ion de-solvation rate. (Nobili et al., 2008) Therefore, metals have been used to coat graphites or other metals. For example, when a commercial graphite anode was coated with silver and/or nickel, the C/D performance of the anode at high charging rate was improved together with much enhanced discharge capacity as can be seen in Figure 12. (Choi et al., 2004)

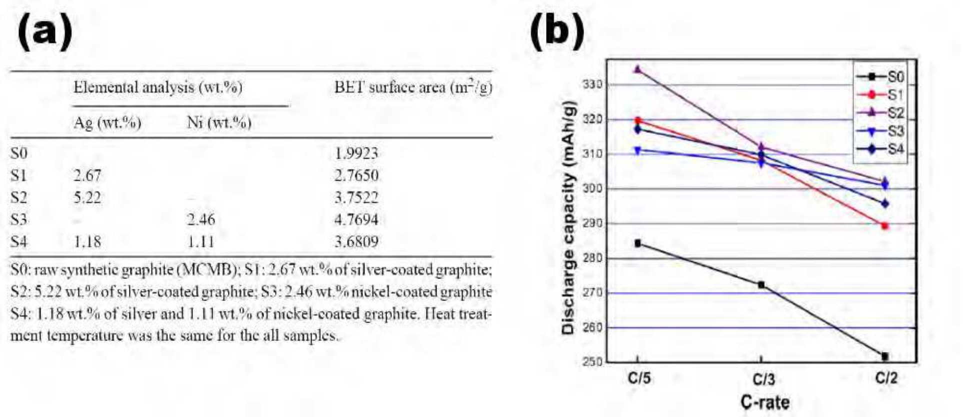

(a)

	Elemental analysis (wt.%)		BET surface area (m^2/g)
	Ag (wt.%)	Ni (wt.%)	
S0			1.9923
S1	2.67		2.7650
S2	5.22		3.7522
S3	-	2.46	4.7694
S4	1.18	1.11	3.6809

S0: raw synthetic graphite (MCMB); S1: 2.67 wt.% of silver-coated graphite; S2: 5.22 wt.% of silver-coated graphite; S3: 2.46 wt.% nickel-coated graphite S4: 1.18 wt.% of silver and 1.11 wt.% of nickel-coated graphite. Heat treatment temperature was the same for the all samples.

Fig. 12. Elemental analysis and BET surface area of metal-coated graphites (a) and effect of metal-coated graphites on maximum discharge capacity at various C-rates. 1M $LiPF_6$ in EC:EMC:DMC (1:1:1) (Choi et al., 2004)

(2) Doping methods

Doping heteroatoms into metal oxide and/or graphite anodes is another effective way to increase electronic conductivity (Chen et al., 2001; Coustier et al., 1999; Endo et al., 1999; Huang et al., 2005; Li et al., 2009; Miyachi et al., 2007; Park et al., 2008; Qi et al., 2009; Santos-Pe et al., 2001; Wen et al., 2008; Zhao et al., 2008) of the LIB anode materials. This surface modification turned out effective particularly for improving the electronic conductivity of metal oxide materials, such as SnO_2 (Santos-Pe et al., 2001), SiO (Miyachi et al., 2007), $Li_4Ti_5O_{12}$ (Chen et al., 2001; Huang et al., 2005; Li et al., 2009; Park et al., 2008; Qi et al., 2009; Wen et al., 2008; Zhao et al., 2008), V_2O_5 (Coustier et al., 1999), and etc, via increased charge carrier density and hopping probability of electrons. Indeed, N-doped $Li_4Ti_5O_{12}$, which was prepared by heat treating $Li_4Ti_5O_{12}$ under NH_3 atmosphere to introduce conductive TiN thin film on the surface, exhibited much enhanced anode performance at high C/D rate as can be seen in Figure 13. (Park et al., 2008) In the various metal (Fe, Ti, Ni)-doped SiO anodes the doped metal formed effective electron conductive path on the active material, which helps fast reversible redox reaction between Si^{4+} and Si at high C/D rates. (Miyachi et al., 2007)

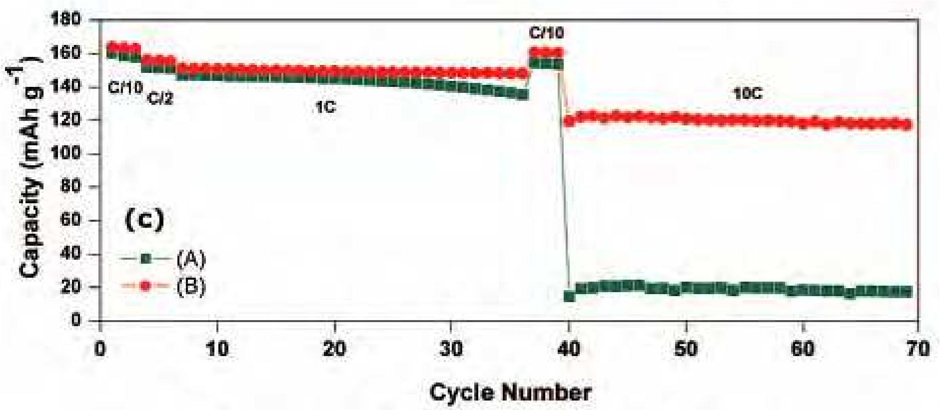

Fig. 13. Reversible capacities of (A) pristine and (B) 10 min-nitridated $Li_4Ti_5O_{12}$ with different charge/discharge current densities during cycling. (Park et al., 2008)

4.1.3 Synthesis of composite active material

The synthesis of composite anode materials has been most commonly adopted to overcome drawbacks of the current LIB anodes, for example, suppression of large volume expansion. (Tarascon & Armand, 2001) This approach was found also effective in enhancing the electron transportation rate. The approaches to synthesizing composites can be categorized into three groups: one is the carbon based composites (Chao et al., 2008; Cui et al., 2009; Gao et al., 2007; Hanai et al., 2005; Ji & Zhang, 2009; Lee et al., 2008; Lee et al., 2000; Lee et al., 2009; Li et al., 2009; Park et al., 2006; Park & Sohn, 2009; Park et al., 2007; Skowronski & Knofczynski, 2009; Veeraraghavan et al., 2002; Wang et al., 2008; Wang et al., 2008; Wen et al., 2008; Wen et al., 2003; Yao et al., 2008; Yin et al., 2005; Yoon et al., 2009; Yu et al., 2008; Zheng et al., 2008), another is the metallic composites (Ahn et al., 1999; Guo et al., 2007; Guo et al., 2009; Hanai et al., 2005; Hibino et al., 2004; Huang et al., 2008; Huang et al., 2005; Vaughey et al., 2003; Wang et al., 2008; Yan & et al., 2007; Yang et al., 2006; Yin et al., 2004; Zhang et al., 2009), and the other is the composites incorporated with conductive addictives.

(1) Carbon based composites

The carbon based composites are of two types: the composite with carbon active material (Cui et al., 2009; Ji & Zhang, 2009; Lee et al., 2000; Park et al., 2006; Park & Sohn, 2009; Park et al., 2007; Skowronski & Knofczynski, 2009; Veeraraghavan et al., 2002; Wang et al., 2008; Wang et al., 2008; Yao et al., 2008) and the composite with carbon conductive material (Chao et al., 2008; Gao et al., 2007; Hanai et al., 2005; Hibino et al., 2004; Lee et al., 2008; Lee et al., 2009; Li et al., 2009; Wen et al., 2008; Wen et al., 2003; Yin et al., 2005; Yoon et al., 2009; Yu et al., 2008; Zheng et al., 2008). In the former case, other conductive materials are used to enhance the electron transportation. If such conductive materials are active with Li ions, like as Co (Wang et al., 2008), Sn (Lee et al., 2000; Park & Sohn, 2009; Veeraraghavan et al., 2002), Sb (Park & Sohn, 2009; Park et al., 2007) and Fe_3O_4 (Cui et al., 2009; Wang et al., 2008), the conductive materials can also play a role as the active material with carbon. As an example of the composite with carbon active material, Wang et al. (2008) prepared a composite of carbon fiber/Fe_3O_4 using electrospinning technique. Because Fe_3O_4 has high theoretical specific capacity of 924 mAh/g and high electronic conductivity, the composite exhibited the specific capacity of about 1000 mAh/g at 200 mA/g of C/D rate.

On the other hand, in the latter case, carbon materials are usually coated on and/or incorporated into the matrix of metallic or insulating or semiconducting active materials. For carbon-coated metal composites, carbon is used as a matrix or template to suppress the volume expansion of and maintain electron pathways in the anode. In this case, metal is the anodic active material, and at the same time, enhance the electron transportation of the carbon material. Indeed, SnSb/C composites synthesized by Park and Sohn (2009) using high energy mechanical milling show the reversible specific capacity of 500 mAh/g over at 2C rate due to enhanced electronic conductivity by SnSb nanocrystallines (see Figure 14)

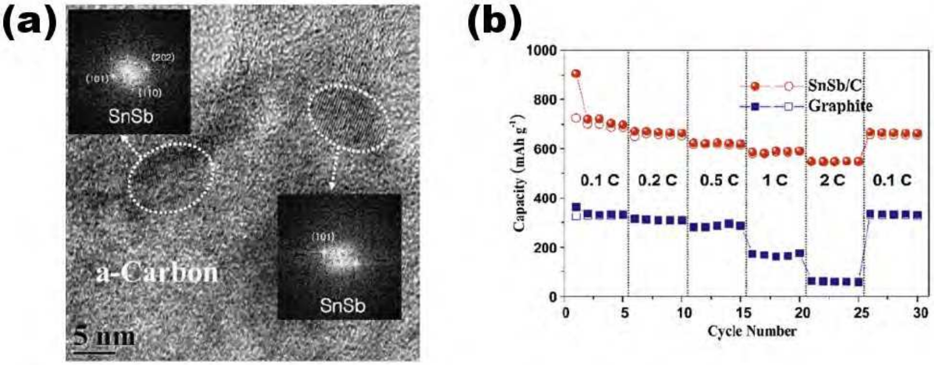

Fig. 14. TEM image with the corresponding lattice spacing of the SnSb/C nanocomposite (a) and the discharge and charge capacity vs. cycle number for the SnSb/C nanocomposite and graphite (MCMB) electrodes at various C rates (SnSb/C: 1C-700 mA/g, graphite: 1C-320 mA/g). (Park & Sohn, 2009)

The carbon-coated insulating materials that have high storage capacity of Li ions, for example, Si (Hanai et al., 2005; Wen et al., 2003), SiO (Chao et al., 2008), $Li_4Ti_5O_{12}$ (Yu et al., 2008), and etc. also show much enhanced anodic performance due to improved electronic conductivity by carbon component in the composite. Indeed, SiO/carbon cryogel (CC) composites showed the specific discharge capacity of 450 mAh/g over at 600 mA/g of C/D rate. This enhanced anodic performance at high C/D rate was attributed to high electronic conductivity and continuous porosity giving increased porosity and improved contact with electrolytes. (Hasegawa et al., 2004) On the other hand, the carbon-incorporated composite system whereby carbon addictives, for example carbon nanotube (CNT) (Lee et al., 2008; Lee et al., 2009; Yin et al., 2005; Zheng et al., 2008), are incorporated into metal oxide system is another simple way to enhancing the electron transportation in the anode system. In this case, there are no additional treatments that may influence the anodic performance of the oxide materials, so this method can thus be applied to the thermally sensitive anode materials. Zheng et al. (2008) used CNTs to increase the high rate performance of CuO anode. As CNTs have high chemical stability, large surface area, strong mechanical strength, and high electronic conductivity, they integrated CNTs and CuO into nanomicrospheres to have enhanced performance at fast C/D rates as shown in Figure 15.